Simultaneous Microwave Photonic Analog-to-Digital Conversion and Digital Filtering

Sitong Wang, Guiling Wu, Feiran Su, and Jianping Chen

***Abstract*— We proposed a scheme which can simultaneously realize photonic analog-to-digital conversion (PADC) and digital photonic filtering for microwave signals. A multi-tap optical pulse shaper is adopted in a photonic sampling and electrical quantizing PADC to change its equivalent channel response, which can be designed and flexibly reconfigured as a finite impulse response digital filter. The principle and operation conditions of the proposed scheme are theoretically analyzed. A system employing an optical time division multiplexing (OTDM)-based multi-tap shaper is demonstrated. Filtering features agreeing well with the theoretical and simulation results are experimentally measured by configuring the path attenuations and delays in the OTDM based shaper.**

***Index Terms*— Digital filters, microwave photonics, optical pulse shaping, photonic analog-to-digital conversion.**

I. Introduction

WITH the development of photonic technology, photonics approaches can bring features difficult or impossible to attain by purely electronic solutions such as high speed, broadband width, simultaneous tuning and reconfigurability, and low jitter [1]. Benefiting from the merits of photonics, microwave photonic filters (MPFs) have been proposed to overcome the electronic analog filters' limitations in bandwidth, loss, immunity to electromagnetic interference (EMI), tunability and reconfigurability [2], [3]. In order to break the bottlenecks of electronic ADCs in bandwidth and aperture jitter, photonic analog-to-digital converters (PADCs) also have been proposed based on the ultra-low jitter and bandwidth features of photonics to realize high precision digitization of high frequency broadband signals [4], [5]. As two basic functions of signal processing, filtering and digitizing are often needed together in many applications, for example, pre-filtering a signal before digitizing for the purpose such as antialiasing, interference suppressing, and phase shifting [6]. Therefore, the schemes able to combine the functions of PADC and MPF can take the advantages of photonics more efficiently for advanced microwave signal processing and receiving. However, till to now, MPF and PADC are almost independently developed. There is still no scheme to combine the functions of PADC and MPF together. Direct cascading an existing MPF and a PADC will suffer from significant loss and distortion for multi-stages electro-optic and optic-electric conversion. We have proposed a photonic scheme to digitize RF signals with a programmable equivalent analog pre-filter by shaping the temporal shape of optical sampling pulses via a programmable wave shaper and a dispersion compensating fiber (DCF) [6], [7]. The sampling pulses are fed into a programmable wave shaper to shape their spectrum and then passed through a DCF to map the optical spectrum of each pulse to its temporal shape through wavelength-to-time mapping. However, the available temporal shaping precision is limited by the programmable wave shaper's resolution and the wavelength dependence of the DCF's dispersion. Therefore, the precision of the filtering frequency response is limited.

In this letter, we propose a simultaneously photonic analog-to-digital converting and digital photonic filtering scheme for microwave signals. Instead of using a wave shaper and DCF based shaper, a multi-tap optical pulse shaper is adopted in the proposed scheme. The wanted filtering frequency response can be achieved and reconfigured simply by adjusting the attenuation and delay of each tap as a digital filter directly. It is worth noting that the digital photonic filtering is not a digital filter, but an analogy filtering before ADC to overcome the limitation of ADCs on system and release the back-end digital processing pressure [2].

II. Principle of Operation

Figure 1 illustrates the diagram of the proposed scheme. A photonic sampling pulse train from a pulse generator is shaped by a multi-tap optical pulse shaper and then modulated by an input RF signal via an intensity modulation. The modulated photonic pulse train is demultiplexed into N "lower" speed sub-trains to release the demand on electric ADCs by an optical demux. Each sub-train is detected by a photodector, and then quantized by an electric ADC. Finally, the sampled RF input is reconstructed according to the multi-channel quantized data by digital processing.

Compared with the pulse shaping scheme in [6], shaping pulses by a multi-tap optical pulse shaper can reach higher precision since adjusting the attenuation and delay of each tap is much easier to be realized with high precision and stability. Therefore, the precision of filtering frequency response can be

Manuscript received October 17, 2017; revised December 29, 2017; accepted December 31, 2017. Date of publication January 4, 2018; date of current version January 29, 2018. This work was supported by the National Natural Science Foundation of China under Grant 61627817 and Grant 61535006. *(Corresponding author: Guiling Wu.)*

The authors are with the State Key Laboratory of Advanced Optical Communication Systems and Networks, Shanghai Jiao Tong University, Shanghai 200240, China (e-mail: wangst@sjtu.edu.cn; wuguiling@sjtu.edu.cn; feiran.su@gmail.com; jpchen62@sjtu.edu.cn).

Color versions of one or more of the figures in this letter are available online at http://ieeexplore.ieee.org.

Digital Object Identifier 10.1109/LPT.2018.2789587

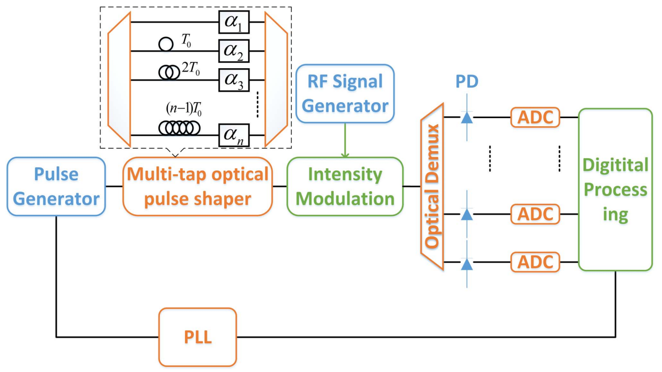

Fig. 1. The proposed photonic scheme. PD, photodector. PLL, phase locked loop.

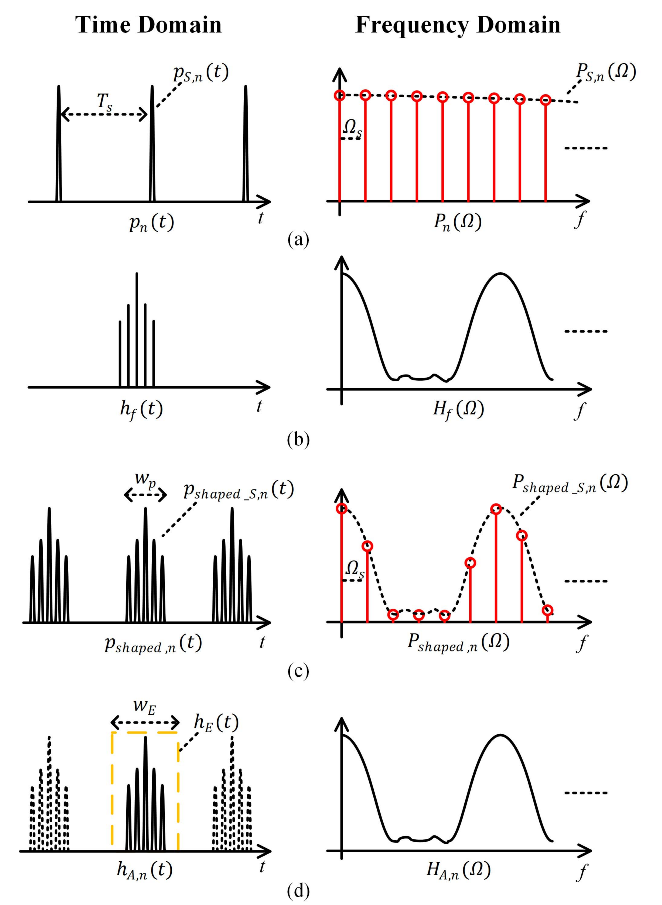

Fig. 2. (a) The temporal shape and spectrum of the n-th sub-train. (b) The time and spectral response of the optical pulse shaper. (c) The temporal shape and spectrum of the n-th shaped sub-train. (d) The impulse response of the n-th sampling channel $h_{A,n}(t)$, and equivalent channel response.

significantly improved. Moreover, the multi-tap optical pulse shaper can be easily designed and reconfigured as a digital filter to achieve the wanted filtering frequency response.

The temporal shape of the n-th sub-train generated by the pulse generator is shown in Figure 2(a), and can be expressed as [8]

$$p_n(t) = P_{A,n} \sum_{m=-\infty}^{\infty} p_{S,n}\left(t - mT_s - d_{p,n}\right) \tag{1}$$

where $P_{A,n}$ is the average power of the pulse train, $p_{S,n}(t)$ is the photonic sampling pulse power normalized by $P_{A,n}$, T_s is the pulse repetition period and d_p is the delay. Its spectrum can be expressed as

$$P_{\mathrm{n}}(\Omega) = \frac{2\pi P_{A,n}}{T_s} \sum_{\mathrm{k}=-\infty}^{+\infty} P_{S,n}(k\Omega_s) \times \exp(-jk\Omega_s d_{p,n})\delta(\Omega - k\Omega_s) \tag{2}$$

which means the envelope of $P_n(\Omega)$ (the black dashed line in figure 2(a)) is proportional to the spectrum of the single sampling pulse $P_{S,n}(\Omega)$, and $\Omega_s = 2\pi/T_s$. Corresponding to the narrow FWHM of the single sampling pulse $p_{S,n}(t)$ and the periodicity of the sampling pulse train $p_n(t)$, $P_n(\Omega)$ is discrete and its envelope has an extremely large bandwidth.

Then the n-th sub-train is shaped by a multi-tap optical pulse shaper shown in Figure 1. Its impulse response is shown in Figure 2(b), and the temporal shape of the shaped pulse train can be expressed as

$$\begin{cases} p_{shaped,n}(t) = p_n(t) * h_f(t) \\ h_f(t) = \sum\limits_{i=0}^{k-1} \alpha_i \delta(t - iT_0) \end{cases} \tag{3}$$

where $h_f(t)$ is impulse response of the multi-tap optical pulse shaper and its spectrum is $H_f(\Omega)$. They can be easily designed and adjusted by altering the weight of each tap α_i and the delay between the adjacent taps T_0.

The shaped sampling pulse train output from the multi-tap optical pulse shaper can be understood as the convolution of the original sampling pulse waveform and the impulse response of the shaper, as shown in Figure 2(c). Every single pulse generated by the pulse generator is shaped as a sub pulse cluster. In the frequency domain, the spectrum of the shaped sampling pulse train is discrete and can be expressed as

$$P_{shaped,n}(\Omega) = P_n(\Omega) H_f(\Omega) \tag{4}$$

Because of the relatively large bandwidth of the envelope of $P_n(\Omega)$, the envelope of $P_{shaped,n}(\Omega)$ is limited by $H_f(\Omega)$.

According to [8], the equivalent impulse response of the n-th channel, $h_{A,n}(t)$, can be expressed as

$$h_{A,n}(t) = -0.5\alpha h_M(t) * \left[h_{E,n}\left(t - d_{E,n}\right) p_{shaped,n}(-t)\right] \tag{5}$$

where α and $h_M(t)$ are respectively the attenuation factor and the impulse response of the intensity modulation, $h_{E,n}(t)$ is the electrical back-end impulse response accounting from the photodector to the electronic ADC on the n-th channel, $d_{E,n}$ is the delay added in the electrical back-end. In Eq. (5), the effect of the modulator is equivalent to a cascade filtering with a relatively large bandwidth, and can be investigated independently. Therefore, the equivalent impulse response of the n-th channel is proportional to the product of the temporal shape of the shaped sampling pulse train and the electrical back-end impulse response.

When the following constraint is satisfied [6]

$$w_p < w_E < T_s \tag{6}$$

where w_p and w_E are the widths of $p_{S,n}(t)$ and $h_{E,n}(t)$ respectively, appropriate $d_{p,n}$ and $d_{E,n}$ can always be found to make the window of $h_{E,n}(t)$ is aligned to one of the pulses of $p_{shaped,n}(-t)$.

Therefore, the equivalent channel response is proportional to the waveform of the single shaped sampling pulse [6], and we have

$$H_{A,n}(\Omega) \propto P_{shaped\_S,n}(\Omega) = P_{S,n}(\Omega) H_f(\Omega) \tag{7}$$

where $H_{A,n}(\Omega)$ is the frequency response of the equivalent channel. Corresponding to relatively large bandwidth of $P_{S,n}(\Omega)$, $H_{A,n}(\Omega)$ is primarily determined by $H_f(\Omega)$.

When all the channels in the system are matched both in gain and delay ($d_{p,n} = (n-1)T_s/N$ and $d_{E,n} = (N-n+1)T_s/N$), the quantized data can be interleaved directly to reconstruct RF input [8]. In such case, the system response, $h_A(t)$, is the same as that of channel 1, $h_{A,1}(t)$. If there exists mismatch among channels, a mismatch correction is needed, which will also make the system response approach to that of single channel.

According to above analyses, one can see that in the proposed scheme we can straightly design the multi-tap optical pulse shaper as a digital filter to achieve a system with the wanted filtering features like filter type, center frequency, passband width, and so on. The design of digital filter is mature while the multi-tap optical pulse shaper with the desired impulse response $h_f(t)$ can be easily obtained and reconfigured by altering the weight of each tap α_i and the delay between of the adjacent taps T_0. It means that a photonic system with a reconfigurable filtering and digitizing will be easily designed and realized.

III. Experimental Setup and Results

The basic principle of the scheme is validated using a single channel system since it can also reflect the response of multi-channel systems with matched or mismatched channel as discussed above. Figure 3 shows the experiment setup of the scheme. A mode-locked laser (MLL) (Precision Photonics, FFL1560) generates a pulse train with a 36.5 MHz repetition rate which satisfies Eq. (6). An OTDM based shaper which contains two 1×16 optical splitters, 16 optical delay lines (ODL) and 16 variable optical attenuators (VOA) is used as the multi-tap optical pulse shaper. These pulses are fed into the first 1×16 optical splitter and split to 16 sub pulse train. In each tap path, an ODL and a VOA are used to control the weight of each tap and the delay between them. After the 16 sub pulse train join together through the second 1×16 optical splitter, each single pulse is shaped as a sub pulse cluster. Each sub pulse cluster has 16 sub pulses with the designed repetition, T_0. In the experiment, the delay between adjacent taps is designed to be $125ps$ and the weight of each tap is alerted to make $h_f(t)$ the same as a 15-order equi-ripple digital filter with a passband cut-off frequency of 0.15GHz, a stopband cut-off frequency of 0.6GHz and a period of 8GHz. A 30 GHz MZM biased at quadrature with a half-wave voltage of 4.5 V is used to modulate the shaped pulse train by the RF signals generated from a microwave signal generator (Rohde & Schwarz, SMF100A). The frequency of the generated RF signal can be controlled by the back-end digitizer. The power level of the RF input is set at 0 dBm to avoid the MZM nonlinearity [9]. The modulated pulse train is detected by a photodector with a 100MHz bandwith and followed by a second-order Butterworth low-pass filter (LPF) with a 74 MHz bandwidth. The photodetected pulse train is finally sampled by a digitizer with an analog bandwidth of 650 MHz and an ENOB of 9.0 (Keysight, M9703A). The synchronizing generated by the MLL is fed into a phase-locked circuit (Texas Instruments, LMK04828) to generate the clocks for the digitizer (42 times of the pulse repetition rate, ~1.53 GHz). The output of the digitizer is then downsampled by 42 to obtain one sample per pulse.

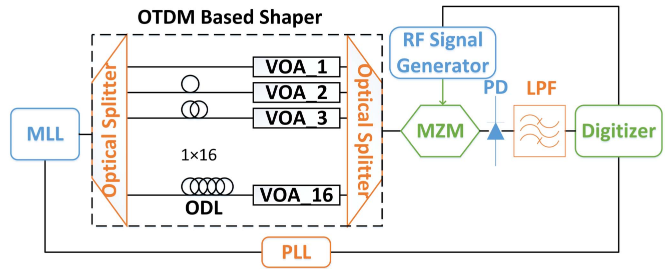

Fig. 3. Experiment setup for the scheme that shaping the sampling pulse by OTDM based shaper to design the channel frequency response.

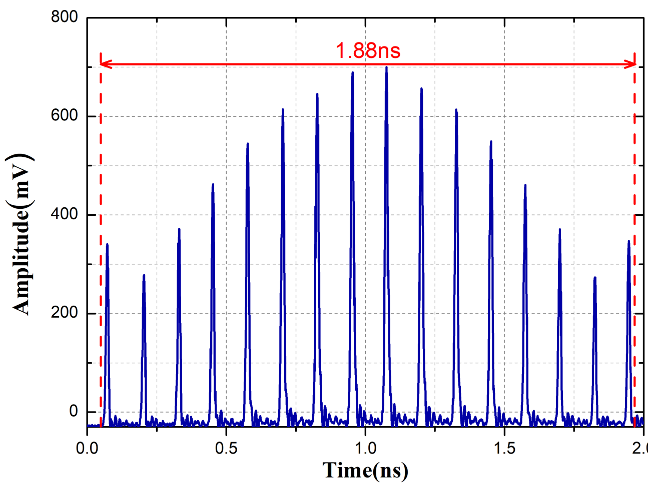

Fig. 4. The temporal shape of the shaped optical pulse.

The measured optical pulse after the OTDM based shaper is shown in Fig (4). The pulse cluster including 16 sub pulses represents an optical sampling pulse. The width of the optical sampling pulse is $\sim 1.88ns$. The measured 1 dB width of the electrical back-end response is $\sim 2.92ns$. Therefore, the constraint condition for the proposed scheme, Eq. (6), is satisfied.

The measured amplitude frequency responses of the system in 0-4GHz and 0-40GHz are shown in Fig 5(a). For comparison, the simulated and the theoretical results are also presented. The filtering responses with the passband cut-off frequency of 0.15GHz, a stopband cut-off frequency of 0.6GHz and a period of 8GHz can be observed, which satisfy with the designed requirements to the 15-order equi-ripple digital filter and are well consistent with the simulated and

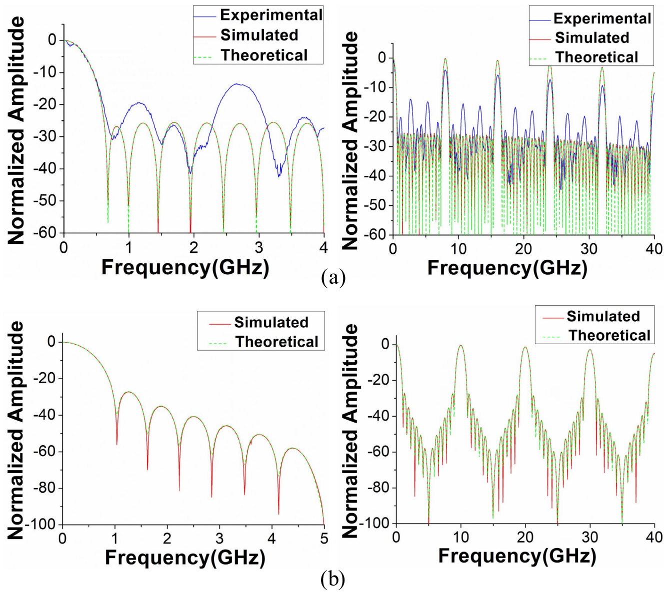

Fig. 5. (a) The amplitude frequency responses of the system in 0-4GHz (left) and 0-40GHz (right) as a 15-order equi-ripple digital filter with a passband cut-off frequency of 0.15GHz, a stopband cut-off frequency of 0.6GHz and a period of 8GHz. (b) The amplitude frequency responses of system in 0-5GHz (left) and 0-40GHz (right) as a 15-order rectangle digital filter with a cut-off frequency of 0.625GHz and a period of 10GHz.

theoretical ones. The relative deviation of 5dB bandwidth between the experimental result and the theoretical one is less than 6%. It indicates a significant improvement in contrast to that (more than 20%) in [6]. The deviation of the experimental result to the theoretical one in stopband may be mainly caused by the link noise in the system.

Fig 5(b) shows the simulated and theoretical system amplitude frequency responses when the impulse response of the OTDM based shaper, $h_f(t)$, is set to a 15-order rectangle digital filter with the cut-off frequency of 0.625GHz and a period of 10GHz by adjusting the delay between adjacent taps to 100*ps* and the weight of each tap to the corresponding value. We can see that the simulated response and the theoretical one are almost coincident, and the designed parameters of rectangle digital filters are reached. It denotes that the system frequency response can be reconfigured flexibly by adjusting the attenuation and delay of each tap in the OTDM based shaper.

IV. Conclusion

We proposed a scheme to simultaneously realize PADC and digital microwave photonic filtering using a multi-tap optical pulse shaper with the wanted filtering frequency response. The wanted filtering features can be simply achieved and flexibly reconfigured by adjusting the attenuation and delay of each tap in the multi-tap shaper as a digital filter with high precision and stablility. A system employing an OTDM based multi-tap shaper is demonstrated. The amplitude frequency responses of system as a 15-order equi-ripple digital filter and a 15-order rectangle digital filter are achieved, respectively. The relative deviation of 5dB bandwidth between the experimental result and the theoretical one can be less than 6%.

References

[1] D. E. Leaird and A. M. Weiner, "Simultaneous broadband microwave downconversion and programmable complex filtering by optical frequency comb shaping," *Opt. Lett.*, vol. 37, no. 19, pp. 3993–3995, 2012.

[2] J. Capmany, B. Ortega, and D. Pastor, "A tutorial on microwave photonic filters," *J. Lightw. Technol.*, vol. 24, no. 1, pp. 201–229, Jan. 2006.

[3] J. Capmany, J. Mora, I. Gasulla, J. Sancho, J. Lloret, and S. Sales, "Microwave photonic signal processing," *J. Lightw. Technol.*, vol. 31, no. 4, pp. 571–586, Feb. 15, 2013.

[4] G. C. Valley, "Photonic analog-to-digital converters," *Opt. Exp.*, vol. 15, no. 5, pp. 1955–1982, 2007.

[5] G. Wu, S. Li, X. Li, and J. Chen, "18 wavelengths 83.9 Gs/s optical sampling clock for photonic A/D converters," *Opt. Exp.*, vol. 18, no. 20, pp. 21162–21168, 2010.

[6] F. Su, G. Wu, and J. Chen, "Photonic analog-to-digital conversion with equivalent analog prefiltering by shaping sampling pulses," *Opt. Lett.*, vol. 41, no. 12, pp. 2779–2782, 2016.

[7] A. M. Weiner, "Ultrafast optical pulse shaping: A tutorial review," *Opt. Commun.*, vol. 284, no. 15, pp. 3669–3692, 2011.

[8] F. Su, G. Wu, L. Ye, R. Liu, X. Xue, and J. Chen, "Effects of the photonic sampling pulse width and the photodetection bandwidth on the channel response of photonic ADCs," *Opt. Exp.*, vol. 24, no. 2, pp. 924–934, 2016.

[9] J. D. McKinney and K. J. Williams, "Sampled analog optical links," *IEEE Trans. Microw. Theory Techn.*, vol. 57, no. 8, pp. 2093–2099, Aug. 2009.